



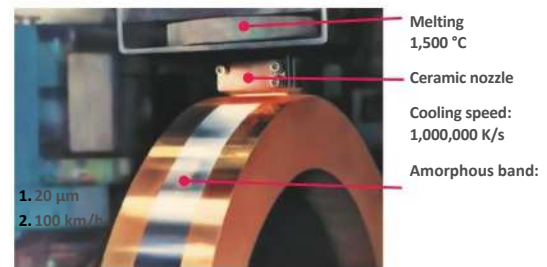
Amorphous cutting strip cores

- | High Saturation Induction
- | Low losses
- | Small build volume
- | Flexible thanks to adjustable air gap

Fe-based amorphous alloys

Amorphous alloys have a disordered atomic structure with no crystalline regions ("grains") or grain boundaries. As a result, they have good a priori prerequisites for soft magnetic behavior, because interference influences such as crystal anisotropy and pinning of grain boundaries are eliminated.

Amorphous Fe-based alloys are produced directly from the melt in a single step in the form of sheets about 23 μm thick in web widths up to about 200 mm. To tune the amorphous (metastable) state, cooling rates of one million kelvin per second are required, even with suitable alloys. This is achieved using rapid solidification technology, in which the melt is pressed through a ceramic nozzle onto a fast-spinning water-cooled copper impeller. These strips are then made into rings, rings or cut strips. In order to reduce internal stresses and adjust the special hysteresis loops, heat treatment is usually performed below the crystallization temperature. It's



with around 500 °C in most commercial administrations within a safe range for many applications. Due to the relatively high magnetostriction, the Fe-based amorphous alloys do not have the excellent magnetic properties of nanocrystalline alloys, but they are distinguished by higher saturation induction and lower costs.

Property	Symbol	Condition	Unit	Value
Saturation induction	Bs	Room temperature (RT)	[T]	1.56
Saturation induction	Bs	130 °C	[T]	1.44
Curie temperature	Tc		[°C]	399
Crystallization temperature			[°C]	508
Maximum operating temperature			[°C]	approx. 130
Magnetostriction	λs		[ppm]	27
Specific electrical resistivity	ρel	Room temperature (RT)	[μΩ·m]	1.3
Density	ρ		[g/cm³]	7.18
Hysteresis losses (magnetization)	PFe	(0.1 T, 25 kHz)	[W/kg]	approx. 15
Hysteresis losses (magnetization)	PFe	(0.3 T, 50 kHz)	[W/kg]	approx. 300

Table 1:
 Material data
 and core
 properties
 (losses)

Mechanical design

The wound and heat-treated cores are impregnated with an epoxy resin system for mechanical stabilization. The amorphous cutting tape cores are therefore a "composite system" with a metal content of approximately 80%.

The different coefficients of thermal expansion **between metal and plastic must be taken into account**, as well as the **typical fluid expansion** of epoxy resins from around 90 °C. Both of these effects can lead to a change in the shape and thus the **air gap**, which changes the **inductance** of the coil.

For **mechanical stabilization**, a **metal clamping band (non-magnetic)** is usually used as well as an **additional gluing of the air gap wedge**. A **contact pressure** of approximately **0.8 N/mm²** between the two halves of the core is recommended.

Reliable mechanical stabilization can also be achieved by a **complete casting** of the coil, for example in an aluminum housing. When flexible **moulding materials** such as **polyurethane (PU) resin**, **operating noise** is also reduced.

The noises are due to **the attractive forces between the two halves of the core** as well as **variations in length and volume due to the magnetostriction** of the material.

If there is a problem, it is recommended to **mechanically disconnect** the core from the **circuit board** or **device housing**.

Amorphous ribbon cores, like **FeSi ribbon cores**, consist mainly of iron and are therefore also **susceptible to corrosion**. This usually only causes an **optical problem**, but **appropriate tests must be carried out**. **Temperature and humidity tests** (also on complete assemblies) can be carried out as a **proposed service**.

The **amorphous tape** becomes **brittle after heat treatment**. When handling the cores, it is imperative to take **protective measures** (goggles, gloves) to avoid loose **splinters**.

The **damaged inner and outer layers** of the tape have no **influence on the magnetic properties**. This damage is unavoidable during the **manufacturing process** and therefore does not constitute a **criterion for rejection**.



Exemple : **Throttle with vertical winding**
52 rpm,
10 x 2.5 mm² with SU 75b cutting tape
chuck for application with
Low ripple frequency

Waist

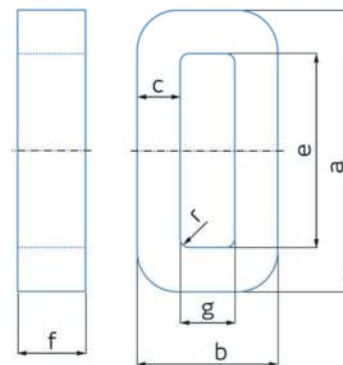
Tolerances and parameters

Amorphous soft magnetic alloy cut strip cores produced by the rapid solidification process are usually offered in the dimensions of the American type AMCC series. In the meantime, the European "IEC 329" types are becoming more and more numerous, for example in the SU series.

Table:
 Designation of dimensions and indication of tolerances according to IEC 329 and for the MCCA-type series

Ribbon cores are windings made of a very thin metal foil, with thickness tolerances and slight differences in surface roughness. As a result, significantly larger tolerances to milled or turned parts inevitably result.

The designation of the different dimensions in this brochure is in accordance with IEC 329. Below you will find a correspondence with the GCCA nomenclature.



Dimensions IEC 329

Designation	IEC 329	AMCC	Tolerance
Outer length	a	(f)	±X
Outer width	b	(e)	±X
Winding height	c	(a)	-X
Window length	e	(c)	min
Core height	f	(d)	±X
Window width	g	(b)	min
Inner winding radius	r	(n.d.)	max

The magnetic parameters are calculated as follows:

Dimensions according to IEC 329

$$A_{Fe, \min} = c_{\min} \cdot f_{\min} \cdot FF$$

$$l_{Fe} \approx a + b + e + g - 1.72 \cdot (r + c/2)$$

$$m_{Fe} = A_{Fe} \cdot l_{Fe} \cdot L$$

MCCA-type series

$$A_{Fe, \min} = a_{\min} \cdot d_{\min} \cdot FF$$

$$l_{Fe} \approx 2 (f_{\max} - 2a) + 2 (e_{\max} - 2a) + \pi \cdot a_{\max}$$

$$m_{Fe} = A_{Fe} \cdot l_{Fe} \cdot L$$

A_{Fe} : cross-section of the iron based on the effect; m_{Fe} :

Nominal weight of the nucleus; l_{Fe} : average length of

the path of the iron; FF : Fill factor ≈ 0.82 ;

ρ : Density = 7.18 g/cm³

Types Series

The following table shows examples of the MCCA and SU series. Stock and other types on request.

Typ	a	b	f		e	g	c		I_{Fe}	A_{Fe}	m_{Fe}	$A_{Cu, 50\%}$	I_{Cu}	O ca.	LI^2 typ
AMCC	[mm] max	[mm] max	[mm]	±	[mm] min	[mm] min	[mm]	±	[cm]	[cm ²]	[g]	[cm ²]	[cm]	[cm ²]	[VAs]
4	52,5	29,5	15	0,5	32,8	10	9	0,5	12,2	1,1	99	1,64	8,8	85	0,08
6.3	55	33	20	0,5	33	11	10	0,5	12,8	1,6	154	1,82	10,4	110	0,12
8	54	36	20	0,5	30	13	11	0,8	13,0	1,8	172	1,95	11,4	120	0,14
10	64	36	20	0,5	40	13	11	0,8	15,0	1,8	198	2,60	11,4	135	0,17
16A	64	36	25	0,5	40	13	11	0,8	15,0	2,3	248	2,60	12,4	145	0,22
16B	74	36	25	0,5	50	13	11	0,8	17,0	2,3	281	3,25	12,4	165	0,26
20	74	36	30	0,5	50	13	11	0,8	17,0	2,7	337	3,25	13,4	170	0,30
25	84	42	25	0,5	56	15	13	0,8	19,4	2,7	379	4,20	13,6	200	0,37
32	84	42	30	0,5	56	15	13	0,8	19,4	3,2	454	4,20	14,6	220	0,44
40	84	42	35	0,5	56	15	13	0,8	19,4	3,7	530	4,20	15,6	235	0,51
50	105	53	25	0,5	70	20	16	1,0	24,4	3,3	586	7,00	16,2	310	0,66
63	105	53	30	0,5	70	20	16	1,0	24,4	3,9	703	7,00	17,2	330	0,75
80	105	53	40	1,0	70	20	16	1,0	24,4	5,2	938	7,00	19,2	350	0,95
100	105	53	45	1,0	70	20	16	1,0	24,4	5,9	1 055	7,00	20,2	370	1,1
125	124	64	35	1,0	83	25	19	1,0	29,2	5,5	1 166	10,4	20,8	460	1,35
160	124	64	40	1,0	83	25	19	1,0	29,2	6,2	1 333	10,4	21,8	495	1,4
200	124	64	50	1,0	83	25	19	1,0	29,8	7,8	1 670	10,4	23,8	540	1,75
250	131	64	60	1,0	90	25	19	1,0	30,8	9,3	2 095	11,25	25,8	595	2,2
320	133	80	50	1,0	85	35	22	1,0	32,8	9,0	2 167	14,9	28,4	700	2,6
400	129	79	65	1,0	85	35	22	1,0	30,2	11,7	2 658	14,9	31,4	780	3,2
500	139	91	55	1,0	85	40	25	1,0	35,0	11,3	2 890	17,00	32,0	850	3,4
630	139	91	70	1,0	85	40	25	1,0	35,0	14,4	3 678	17,00	35,0	930	4,0
800A	139	91	85	1,5	85	40	25	1,0	35,0	17,4	4 466	17,00	38,0	1010	4,6
800B	159	101	85	1,5	95	40	30	1,0	39,0	20,9	5 972	19,00	39,0	1175	5,7
1000	176	107	85	1,5	105	40	33	1,0	42,2	23,0	7 109	21,00	39,6	1290	6,4
SU	[mm] max	[mm] max	[mm]	-	[mm] min	[mm] min	[mm]		[cm]	[cm ²]	[g]	[cm ²]	[cm]	[cm ²]	[VAs]
75b	128,6	75	41,1	1,1	78	25	24,7	1,0	27,9	7,7	1 539	9,75	23,2	550	2,2
90a	155,8	90	30,9	1,4	95	30	29,6	1,1	33,9	6,9	1 678	14,25	24,1	700	2,8
90b	155,8	90	50,9	1,4	95	30	29,6	1,1	33,9	11,6	2 824	14,25	28,1	800	4,8

Table: Mechanical and magnetic ratings/standards of standard types. O is the casing surface of a coiled cutting tape core without the base surface. The LI^2 energy product can vary greatly depending on the application. Below you will find explanations and information about these settings.

Notes on the use of chokes

Strip cores cut from Fe-based amorphous alloys offer an attractive combination of high saturation induction and low losses. This makes them particularly suitable for PFCs or storage coils in power applications.

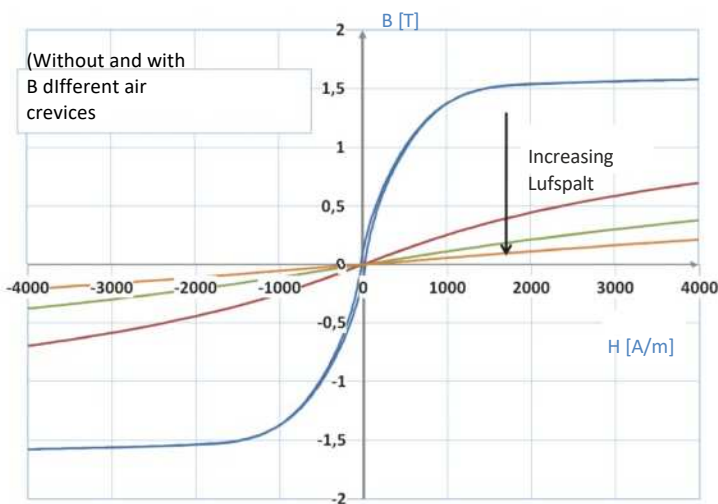


Fig. 3: Typical characteristic curve B(H) of amorphous cut band cores

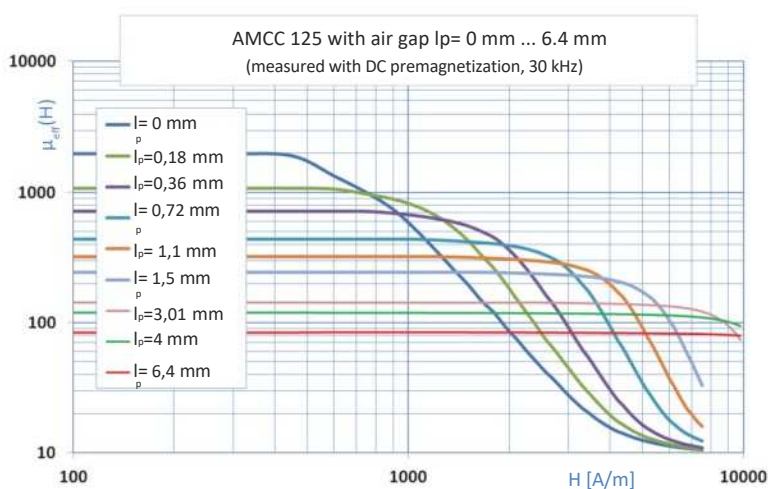


Figure: Typical effective permeability for different air spaces

In the design of the coils, it is exploited that the inductance L is proportional to the square of the number of turns N , but that the field strength H in the nucleus increases only linearly with the number of revolutions.

Materials with low permeability (i.e. high field strengths without the core becoming saturated) are used and the desired inductance L is defined by the number of revolutions.

Amorphous materials are highly permeable, so the current load capacity of stop coils with amorphous cutting belt cores is adjusted via an air gap insert.

The characteristic "no air gap" curve was measured on a core cut without an air gap insert. By widening the air gap the characteristic curve is increasingly "sheared" and the current load capacity increases.

As the air gap increases, the effective permeability decreases and the current carrying capacity increases. A higher number of revolutions is required to reach the target inductor. In addition, the

Additional losses in the core and winding due to current displacement and field distortions.

Size Notes

Small sizes (and thus low costs) are achieved through maximum use of the copper winding chamber with maximum control at the same time.

The **energy storage capacity** E_{choke} , or the energy stored in an inductor, is defined by the inductance L and the square of the current.

It corresponds to the work required to magnetize the inductor:

$$E_{\text{choke}} = \frac{1}{2} \cdot L \cdot I^2$$

This relationship remains valid as long as the **inductor** or the **magnetic core** operates within the linear region, i.e., before saturation.

For storage inductors or PFC inductors, the following relation between $L \cdot I^2$ and the magnetic characteristics of the core can be derived:

$$L \cdot I^2 \approx S_{\text{eff}} \cdot A_{\text{Cu}} \cdot A_{\text{Fe}} \cdot \hat{B}_{\text{max}}$$

In this analysis, the term I_L^2 results from two components:

- the **maximum thermal current capability** $I_{\text{eff,max}}$ (RMS value), and
- the **maximum magnetic current** $I_{\text{B,max}}$ (peak value), without driving the core into magnetic saturation (drop in inductance).

The corresponding quantities in the formula are:

- the **current density** S_{eff} ,
- the **maximum magnetic flux density** \hat{B}_{max} of the core material,
- and the **effective permeability** μ_{eff} , determined by the air gap.

The **maximum current density** depends on the component size, the cooling conditions, and the copper losses. These losses consist of the **ohmic component**, as well as additional losses caused by **skin effect**, **proximity effect**, and **field-leakage influences** due to the air gap.

The corresponding relationships and design methods are relatively complex. Nevertheless, the following chapter attempts to provide simplified empirical formulas that enable quick **pre-dimensioning**.

Due to the large variety of practical applications, thorough **experimental validation** is indispensable. We explicitly state that we do not assume any guarantee or responsibility regarding the accuracy of these approximate formulas.

Definition of currents in chokes

The maximum values of the RMS current and the peak current are the basic parameters for the thermal and magnetic design of the throttle

The currents provided are those that consist either of a DC component with current ripple or of a 50–100 Hz fundamental frequency with a superimposed higher-frequency ripple current. The maximum peak current as well as the maximum RMS current must be taken into account for energy-storage chokes.

$$\hat{I}_{\max} = I_{N,DC} \cdot \sqrt{2} + \frac{I_{R,SS}}{2}$$

$$I_{\text{eff,ges}} = \sqrt{\left(I_{N,DC}\right)^2 + \left(\frac{1}{\sqrt{2}} \cdot \frac{I_{R,SS}}{2}\right)^2}$$

For PFC chokes:

$$\hat{I}_{\max} = I_{N,eff} \cdot \sqrt{2} + \frac{I_{R,SS}}{2}$$

Additional ripple frequencies must be taken into account accordingly.

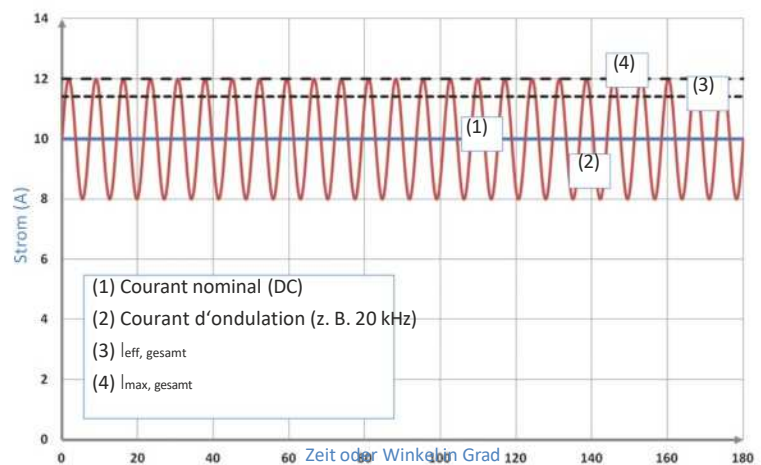


Figure : Courants dans une bobine de stockage (schéma)

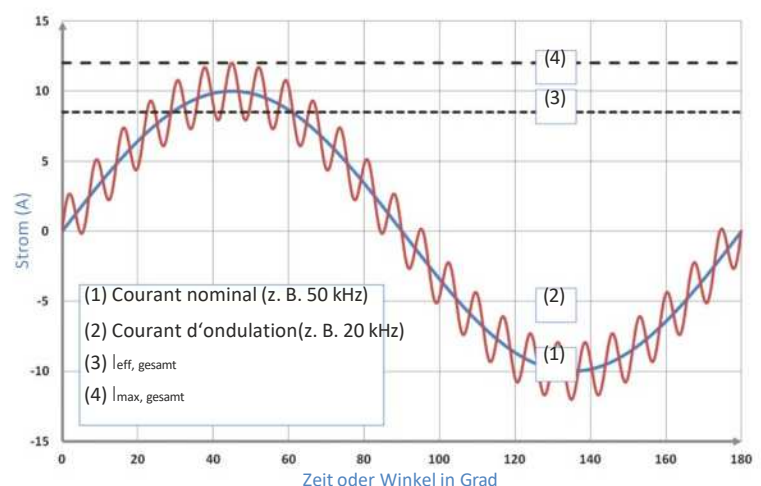


Figure : Courants dans une bobine PFC (schéma)

Estimation du gain maximal

Maximum throttle control depends on the induction of the material sawing of the drop in permeability or inductance with the current load.

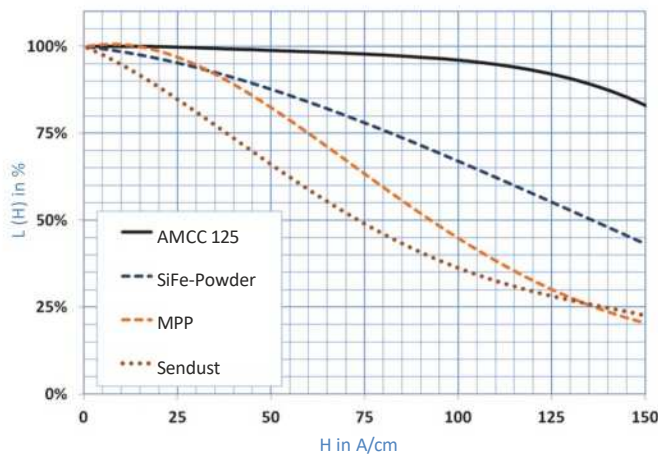


Figure : Dependence of the inductor on the Testing of different accelerator materials with μ_{eff} permeability ≈ 60 (typical behavior)

An advantage of amorphous strip cut nuclei with air gap over powder nuclei is a significantly greater decrease in inductivity as excitation increases. This makes it possible to achieve volume-optimised chokes with greater "rigidity".

The maximum energy of a choke is at the highest point of the curve

$$E = \frac{1}{2} \cdot \mu_0 \cdot \mu_{eff}(H) \cdot H^2 \cdot V.$$

At this point, the permeability or inductivity has dropped by about 30% compared to its initial value and, due to the characteristic steep drop of amorphous nuclei, is already relatively close to saturation induction. A more conservative design is around a decrease in inductivity of about 20%.

This value results (with a relatively low dependence on geometry and air gap) from the representation

$$B = \mu_0 \cdot \mu(H) \cdot H.$$

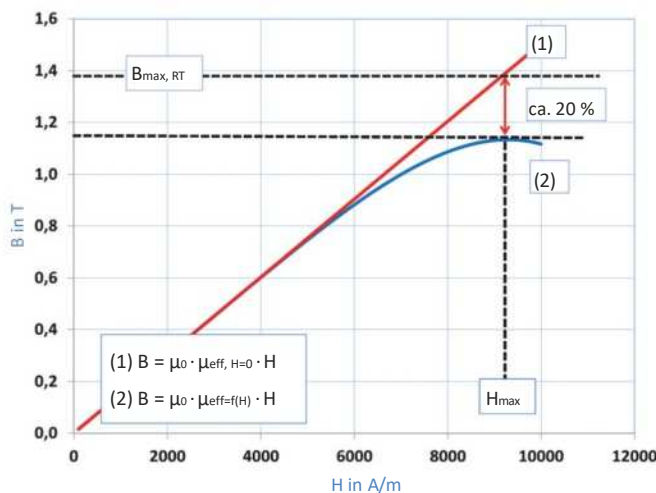


Figure: Typical "near" saturation behavior of amorphous cut band nuclei with μ_{eff} air gap, $H = 0$ is the permeability of the effect within the linear range defined by the air gap.

If we use differential permeability (instead of physically correct absolute permeability) for $\mu(H)$, we obtain a "virtual" maximum of B corresponding to this decrease of about 20% in permeability. Without this decrease in permeability, the nuclei would be excited to about 1.3 T at this point.

This relationship is illustrated in the figure. As a first approximation, we can therefore speak of a theoretical "optimal excitation" of about 1.4 T at room temperature, or approx. 1.3 T at temperatures between 120 and 130 °C. This allows — regardless of the usual differences between the characteristic sets for each core material and the air gap variants — a direct estimate of the maximum effective permeability for the maximum applied current as a function of the number of turns N (or vice versa): \hat{I}_{max}

$$\hat{I}_{max} \approx 1,3 \text{ T} = \mu_0 \cdot \mu_{eff} \cdot \frac{N \cdot \hat{I}}{l_e}$$

Determination the number of laps

The optimal number of revolutions for a given inductance should be as low as possible in order to exert as little thermal stress as possible on the winding without magnetically driving the core.

As indicated, an approximate calculation can be made with a maximum induction of 1.3 T assuming constant permeability. This makes it possible to estimate the number of turns "magnetically" possible. $\hat{B}_{max} N_{mag}$

From the available cross-section of the conductor, it is possible, depending on the ampacity density, to calculate the maximum number of turns "thermally" possible for a concrete application case. $A_{Cu} S_{eff} N_{therm}$

These relationships are represented in the figure as a function of the air gap (and therefore the effective permeability). As you would expect, there is an optimal range for the energy density of a choke. The optimal number of turns for a given core dimension results when the core is neither magnetically nor thermally overloaded.

$$N_{mag,max} = \frac{B}{\mu_0 \cdot \mu_{eff} \cdot \frac{I_{fe}}{l_e}}$$

$$N_{therm,max} = \frac{A_{Cu}}{l_{eff,cu} \cdot S_{eff}}$$

If we set , the following relation follows: $N_{opt} = N_{mag,max}$

$$\mu_{eff} = \frac{B}{\mu_0 \cdot I_{max} \cdot \frac{I_{fe}}{A_{Cu}}}$$

For , 1.3 T can be used. If linear behavior is required, lower values should be used. \hat{B}_{max}

The current density remains as "unknown". Typical current densities range from approx. < 1 A/mm² for high currents and natural convection, to approx. 5–10 A/mm² for lower currents and additional cooling measures. S_{eff}

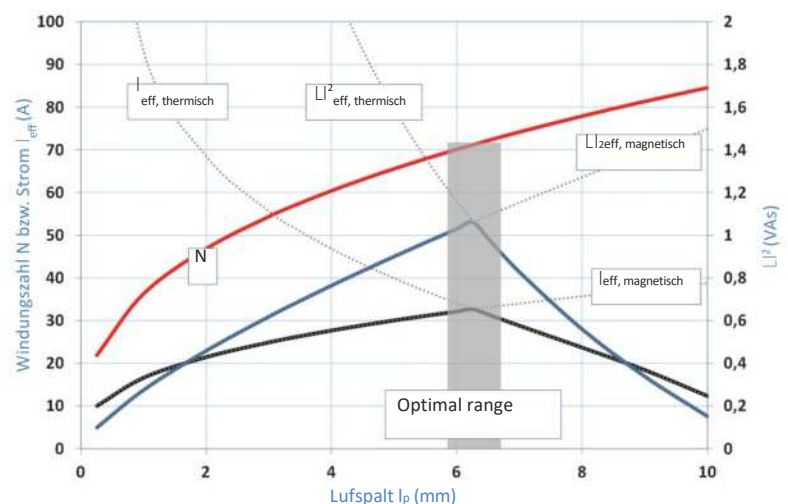


Figure : Estimation of the thermal and magnetic currents allowed for a PFC choke with AMCC 125 core and L = 0.6 mH. Assumptions: current ripple of about 20% with f = 20 kHz, overheating of about 75 K

You can use either empirical values or an estimated initial value for the current density with the following approximation (for natural convection):

$$S_{\text{eff}} \approx \sqrt{\frac{v \cdot O \cdot \Delta T}{c_1} + \frac{O}{c_2}} \cdot c_1 \cdot \rho_{\omega} \cdot l_{\omega} \cdot A_{\omega}$$

S_{eff} : effective current density in A/m²

v : share of copper losses in total losses, e.g. 0.5 for equal parts, e.g. 0.7 for a "copper-oriented" design

O : envelope area of the choke without the bottom, in m²

ΔT : supertemperature in K for natural convection

ρ_{ω} : specific electrical resistivity of the winding (copper or aluminium) in Ωm

l_{ω} : average length of the current path in m (see Table 3)

A_{ω} : effective surface area of the conductor in m² (see Table 3)

k_{Wv} : correction factor depending on the frequency and the type of wire for copper losses. Typical values: approx. 2–3 at 20 kHz (see chapter "Losses and overtemperature")

c_1, c_2 : correction factors from the empirical relationship for overtemperature as a function of envelope area and losses. $c_1 \approx 0.1 \text{ m}^2/\text{W}$ and $c_2 = 1 \text{ K}$ (K = Kelvin)

With an initial value chosen for and the effective permeability calculated from it, we can then determine: $S_{\text{eff}} \mu_{\text{eff}}$

$$N \approx \frac{B}{\mu_0 \cdot \mu_{\text{eff}}} \cdot \frac{l_e}{I_e}$$

the number of turns permissible from the magnetic point of view, then check whether the desired inductivity L is reached:

$$L \approx N^2 \cdot \mu_0 \cdot \mu_{\text{eff}} \cdot \frac{A_{\text{Cu}}}{l_e}$$

The air gap l_k (= total air gap) can be approximately estimated from the effective permeability. The following formula has been interpolated from measurements on different MCCA types and can be used to determine an initial value, which will however need to be verified empirically:

$$l_k \approx l_{\text{Fe}} \cdot c \cdot \left(\frac{\mu_{\text{eff}}}{\mu_0} - 1 \right)^{\frac{1}{b}}$$

with:

$a \approx 1.9$ (range approx. 1.5... 3)

$b \approx -0.7$ (range approx. -0.6... -0.8)

$c = (\text{cm}) / (\text{cm}^2)^{\frac{l_{\text{Fe}}}{A_{\text{Fe}}}}$

If the desired inductivity L is well achieved, the current density can be reduced or a smaller core can be used. Conversely, if the current density is to be increased, a larger core will need to be used. S_{eff}

A disadvantage of larger air gaps is the increase in copper and iron losses due to leakage fields. If the choke is controlled too close to saturation, the current and voltage are distorted by the decrease in inductivity.

First, the heat load corresponding to the chosen current density must be estimated. The loss mechanisms are relatively complex and depend strongly on the concrete structure of the winding, the air gap and the cooling possibilities. The approximation formulas described in the next chapter can therefore be used as a reference or guide.

Losses and overheating

Copper losses depend on the frequency and specific winding structure, copper and core losses also depend on the air gap due to the influence of the parasitic field. The following formulas can be used to approximate the superheating due to copper and core losses.

Copper losses consist of ohmic parts as well as frequency-dependent losses caused by skin effects and proximity effects:

$$P_{cu} \approx \left(\rho_{\omega} \cdot \frac{l_{\omega} \cdot N^2}{A_{\omega}} \cdot I_{eff}^2 \right) \cdot K_{w \approx v}$$

The correction factor depends on the frequency, the type of wire used (litz or solid wire), and the concrete structure of the winding (single or multilayer). In the mid-frequency range around 20 kHz, typical values of 2 to 3 are common. $K_{w \approx v}$

For nucleus losses in amorphous cores cut into bands, the following approximation formula can be found in the literature, valid for the range of approx. 10–30 kHz, for low excursions (10–30% ripple) and without air gaps:

$$P_k \approx m_{Fe} \cdot 6,5 \cdot f^{1,51} \cdot \hat{B}_{ripple}^{1,74}$$

The frequency **f** must be entered in **kHz**, the mass **mFe** in **kg** and in **B**tesla. This results in a value in **watts**.

In the literature, we find for chokes using amorphous kernels cut into strips the following approximation formula for supertemperature:

$$\Delta T \text{ [K]} \sim \left(\frac{c_1 \cdot P_{\text{Gesamt}}}{O} \right)^{0,85} \cdot c_2$$

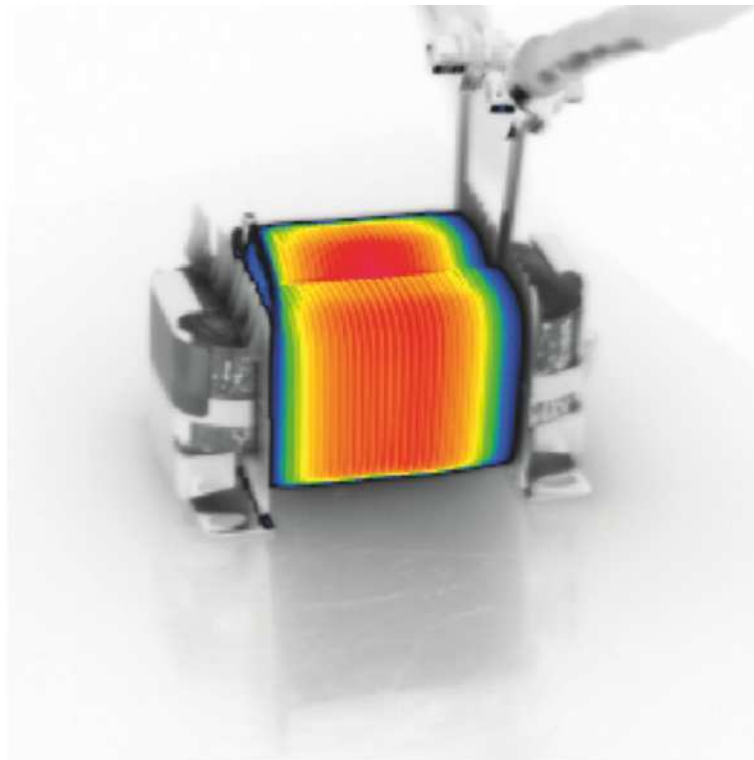
Here, **O** is, in this approximation, the envelope area of the choke without the bottom, in m². The corresponding approximate values can be found in the table.

P_{Gesamt} represents the total losses in watts (W).

In addition, we have:

$c_1 = 0.1 \cdot \text{m}^2/\text{W}$ and $c_2 = 1 \cdot \text{K}$ (K = Kelvin).

Experimental verification is essential, because depending on the construction and environmental conditions, significantly higher temperatures can be achieved.



Thermal imaging of a 7.1 x 2 mm² vertical copper coil choke shows a thermal overload at an effective current of 52 A. In this example, the thermal current value calculated using the formulas was about 10 to 20 percent too high.

Bobbins and tension strips

To match the types of cores listed, we offer coil formers and clamping straps. The coil formers are made of fiberglass-filled polyamide 66 (nylon). The dimensions are listed in the table.

Typ	A	B	C	D	E	F	G
AMCC 20	51	47	12	24	44	30,5	1,8
AMCC 32	57	53	14	28	49	30,5	2,5
AMCC 50	71	67	17	36	49	25,5	2,5
AMCC 80	71	67	17	35,5	63	41	2,5
AMCC 100	71	67	18	35,5	70	47	2,5
AMCC 125	84	79,2	20	40	54	35,5	2,5

Table: Nominal dimensions of standard coils (in mm)

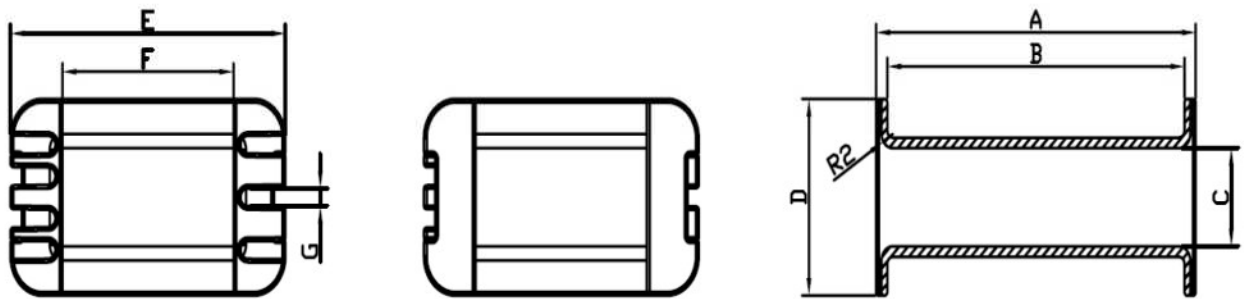
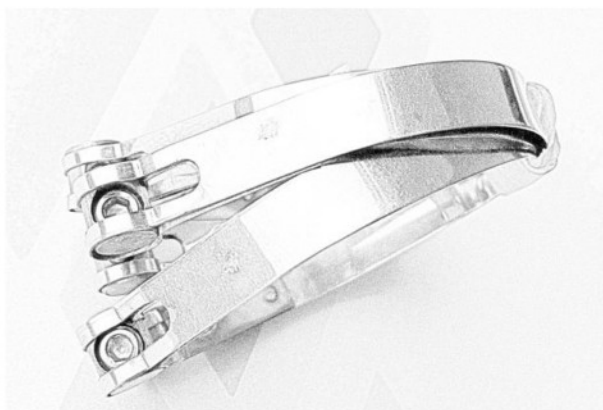


Figure : Sizing of coil formers



We offer non-magnetic steel tension straps in a 6.2 mm bandwidth and closure with Allen screws.

Figure: Tension Straps

Terms and definitions

Below is a summary of the formula symbols used with a brief description.

Table of Symbols, Units and Descriptions

Symbol	Unit	Description
B	T (Vs/m ²)	Magnetic flux density (induction)
H	A/m	Magnetic field strength
μ_{eff}	—	Effective magnetic relative permeability
μ_0	Vs/Am	Magnetic constant ($4\pi \cdot 10^{-7}$)
B _s	T	Saturation induction
T _C	°C	Curie temperature
λ_s	ppm	Saturation magnetostriction
ρ_0	$\Omega \cdot \text{m}$	Specific electrical resistivity
ρ	kg/m ³	Specific material density
A _e	m ²	Effective magnetic cross-section
l _e	m	Mean magnetic path length
FF	%	Ratio of magnetic to geometric cross-section
A _{Cu}	m ²	Effective copper cross-section
l _j	m	Mean turn length
O	m ²	Enclosure surface area of the choke
E _{drossel}	VAs	Energy stored in the choke
L	H	Inductance of the choke
\hat{I}	A	Maximum peak current
I _{eff}	A	Effective (RMS) current
N	—	Number of turns
S	A/m ²	Current density
l _p	m	Total air gap
P _{Cu}	W	Copper losses
P _{Fe}	W	Iron losses
K _{w,l}	—	Correction factors (copper / total losses)
V _{eff}	m ³	Effective core volume